

Electronic Supplementary Information (ESI):

# Strain-induced Multigap Superconductivity in Electrene Mo<sub>2</sub>N: A First Principles Study

Zenner S. Pereira<sup>a\*</sup>, Giovanni M. Faccin<sup>b</sup>, and E. Z da Silva<sup>c†</sup>

<sup>a</sup>Departamento de Ciência e Tecnologia, Universidade Federal Rural do Semi-Árido (UFERSA), CEP 59780-000, Campus Caraúbas-RN, Brazil.

<sup>b</sup>Faculdade de Ciências Exatas e Tecnológicas, Universidade Federal da Grande Dourados - Unidade II, CP 533, 79804-970, Dourados - MS, Brazil.

<sup>c</sup>Institute of Physics "Gleb Wataghin", UNICAMP, CP 6165, 13083-859, Campinas - SP, Brazil.

## 1 Band structure and Fermi Surface.

Figure S1 shows how Wannier band structure fits DFT results for the relaxed monolayer of Mo<sub>2</sub>N. The Complete band structure and respective Fermi Surface (FS) of relaxed and stressed monolayer by 3% biaxial strain are shown in Figure S2. Each band crossing Fermi level is colored and labeled. The corresponding FS is shown in the right side panel. The figure S2 helps to understand how band structure and FS are modified by applied strain as discussed in the main article.

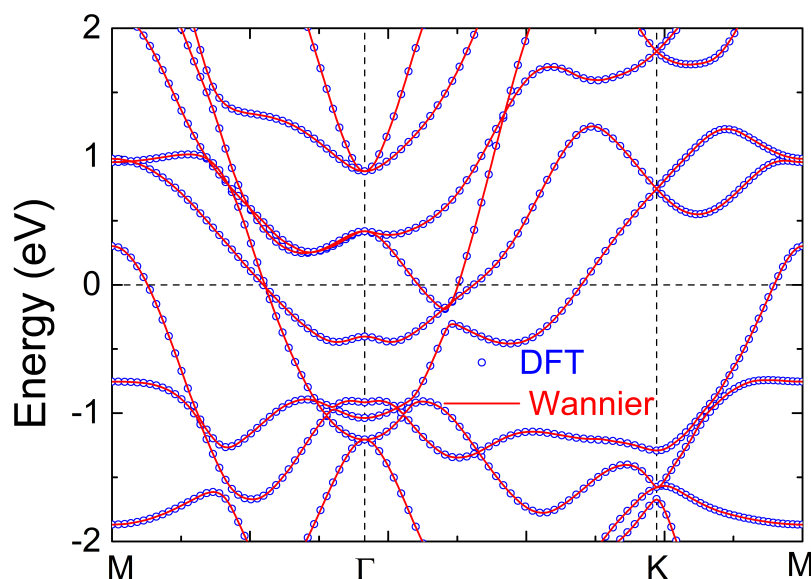


Figure S1: Band structure for relaxed monolayer obtained from DFT calculation (blue) and interpolated bands by wannierization (red).

We also studied the spin-orbit coupling (SOC) effect on the electronic band structure. Figure S3 shows that the band structure is almost not affected by the SOC effect over all biaxial strain simulated. As a consequence, we expect that SOC has very little effect on the EPC parameter and other superconductivity properties. Simulations present in this work do not include SOC effects.

\*Corresponding author: zenner.silva@ufersa.edu.br

†Corresponding author: zacarias@ifi.unicamp.br

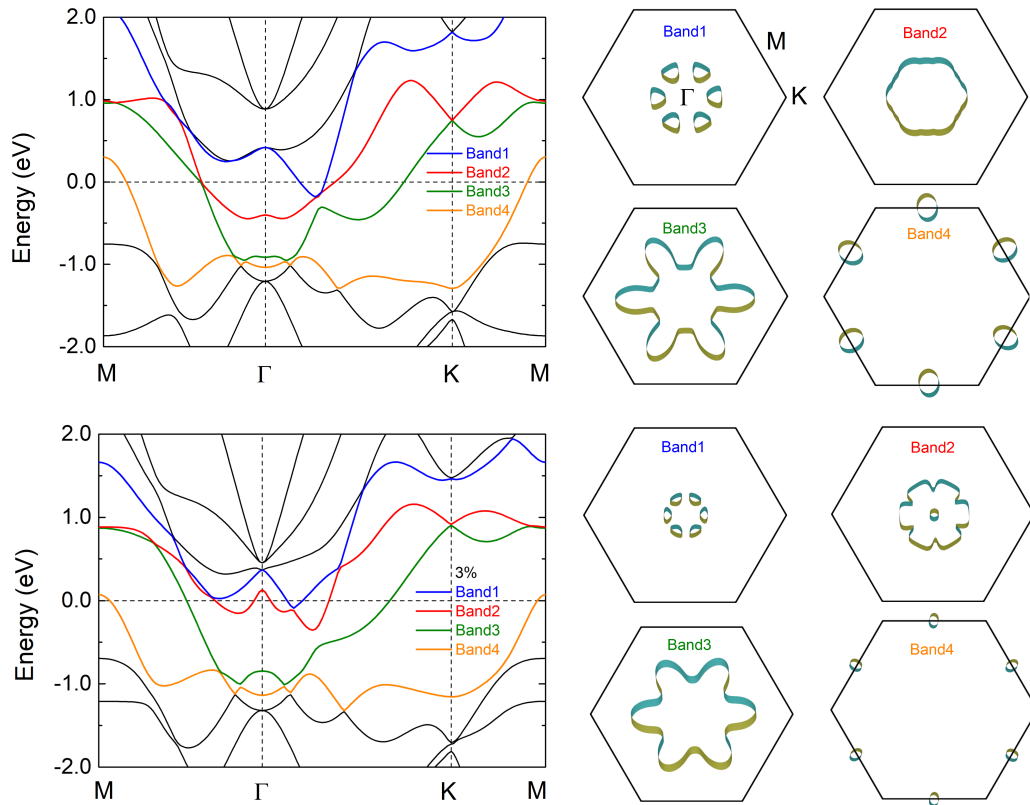


Figure S2: Electronic band structure for relaxed (top panel) and 3% strained (bottom panel) structures. Respective FS for each colored band are in the right side. Colors in the FSs are only used to distinguish the internal and external sides of the surface and help visualization. Figures for FSs were adapted from VESTA package (<https://jp-minerals.org/vesta/en/>).

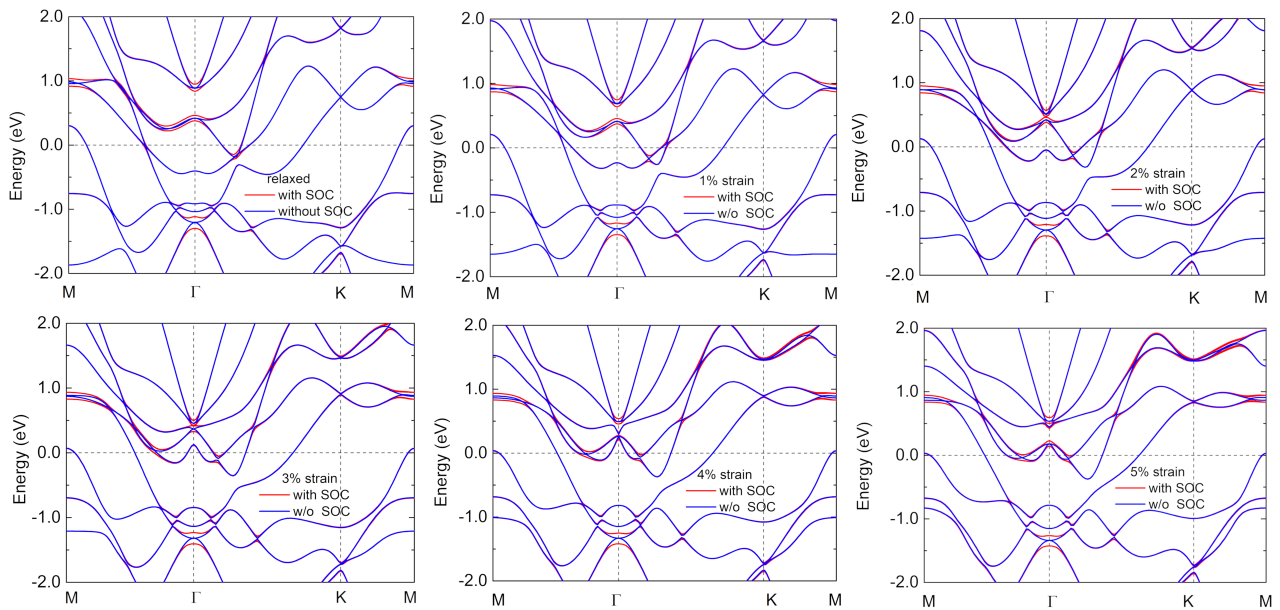


Figure S3: Band structures with SOC correction (red) and without SOC (blue).

## 2 Electron-Phonon Coupling and Anisotropic GAP.

Figure S4 shows isotropic Eliashberg spectral functions and how Electron-Phonon Coupling (EPC) strength ( $\lambda$ ) is modified by biaxial strain. The contribution to  $\lambda$  was divided in acoustic and optical parts. In Figure S5 the phonon dispersion and the phonon-self energy are displayed. The blue lines are colored with red circles proportional to phonon-self energy for each phonon mode. Figure S4 and Figure S5 indicate the behavior of acoustic and optical modes as discussed in the main article. It is also important to point out that the lower acoustic K-M line at 5% strain indicates stability and a high partial EPC parameter. However, when strain is increased above 5%, the same line is the main source of mechanical instability for 2D Mo<sub>2</sub>N. Figure S6 resumes how  $T_c$  changes for McMillan model, isotropic and anisotropic ME formulations.

Figure S7 shows isotropic and energy distributions of the anisotropic superconducting gap as a function of temperature for strained monolayers at 1%, 2%, 4% and 5%. Respective FSs are shown just below the gaps figures. At 1% strain, changes in the band structure are not enough to create a new gap. However, at 2%, a new and very small isolated  $\Delta_k$  distribution with higher energy distribution can be observed. That results from the modified band2, which is very close to Fermi level around  $\Gamma$  point. It is important to note that ME equation is solved to take into account 1.0 eV within the Fermi surface window, that is enough to guarantee interaction close to Fermi level. The effect is intensified as strain is increased. At 5% this new  $\Delta_k$  overlaps with the other distributions with lower energy gap.

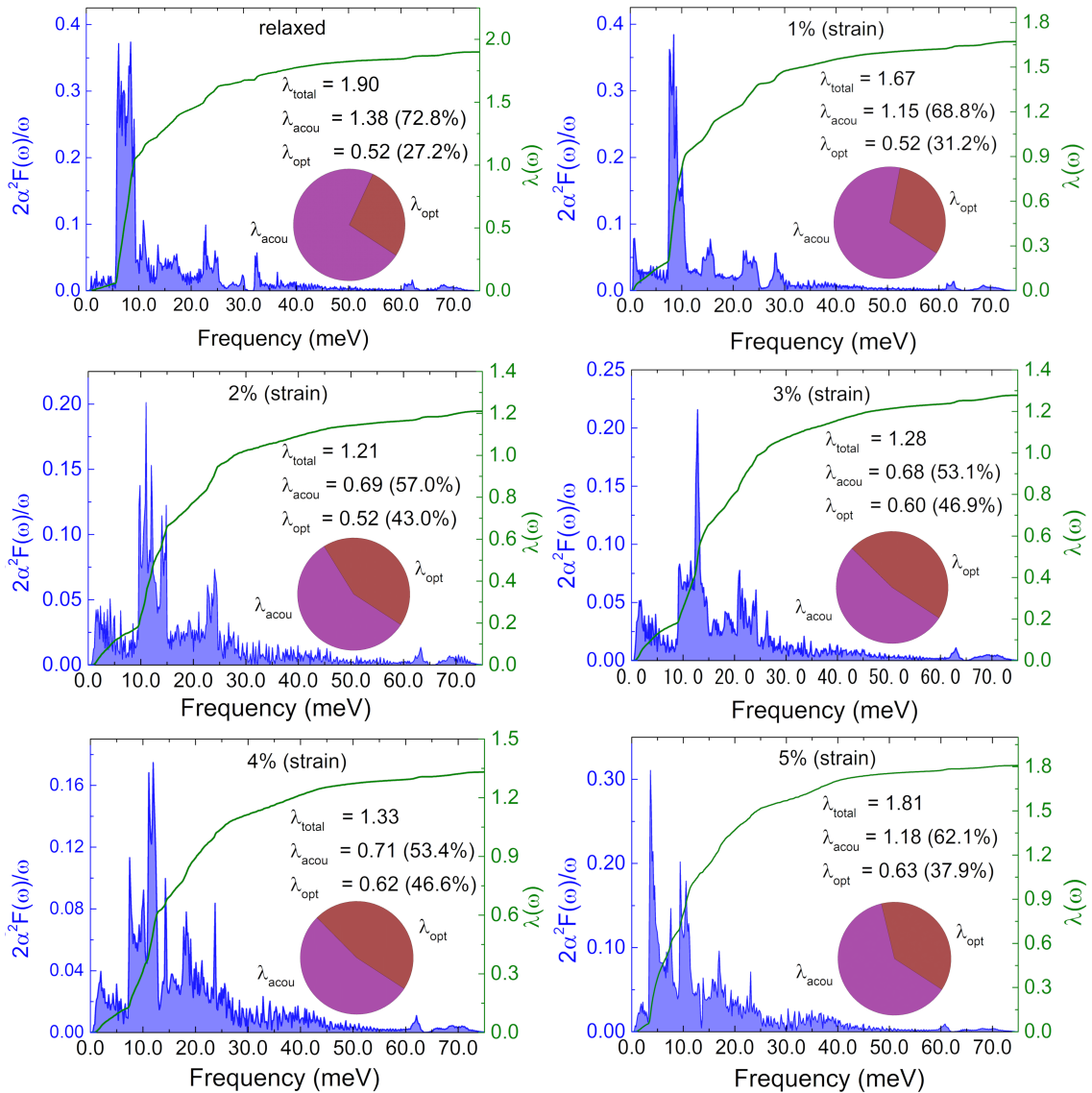


Figure S4: Isotropic Eliashberg spectral function ( $2\alpha^2F(\omega)/\omega$ ) and integrated EPC parameter in the range from 0 – 5% biaxial strain. The percentage of acoustic and optical phonon contributions are featured in a pie chart.

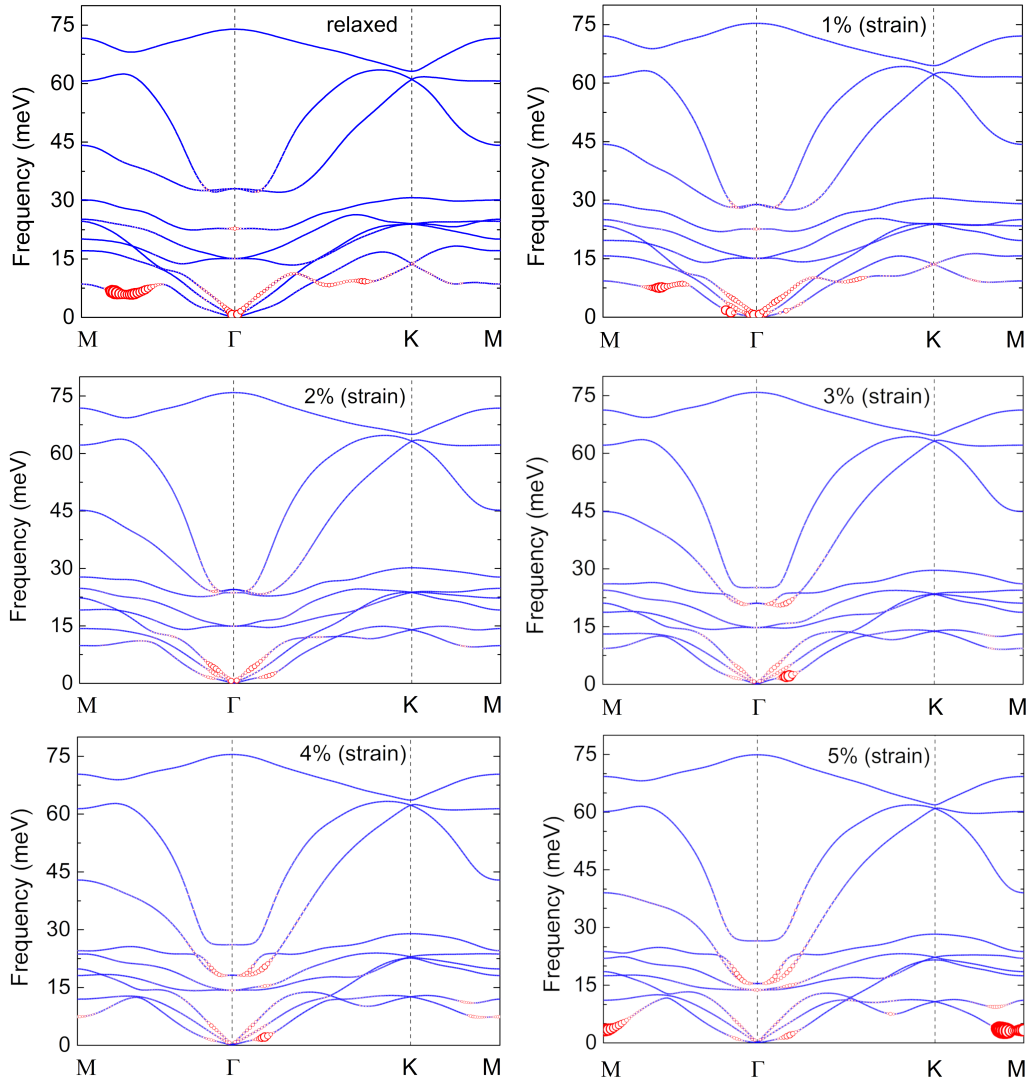


Figure S5: Phonon curves and phonon-self energy in the range from 0 – 5% biaxial strain. Lines are colored in blue. Red circles are proportional to the phonon-self energy of each phonon mode.

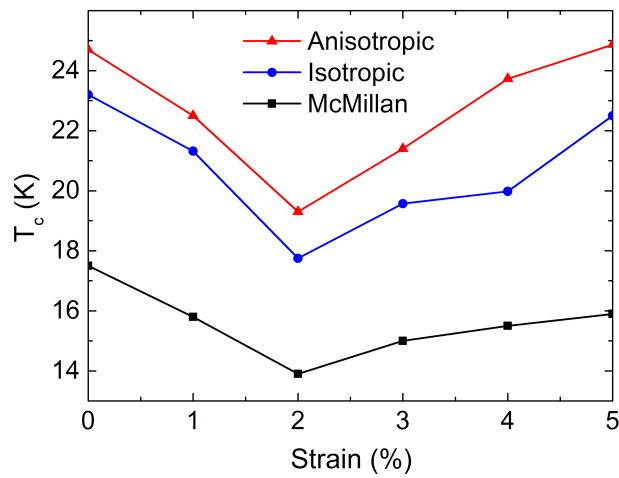


Figure S6:  $T_c$  values versus strain for McMillan-Allen-Dynnes model (black line), isotropic (blue line) and anisotropic (red line) ME formulations.



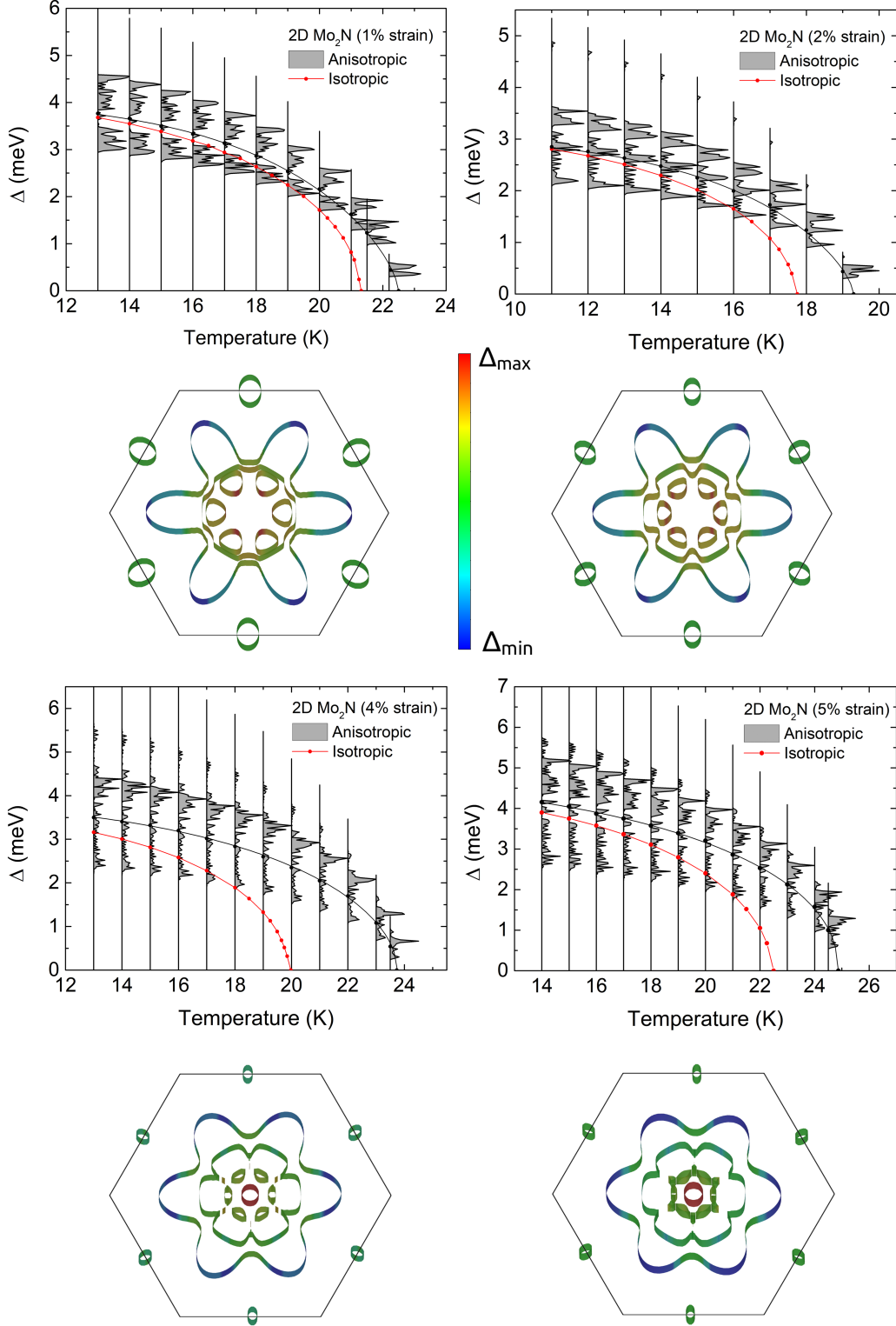


Figure S7: Computed isotropic gap (red line) and energy distribution of the anisotropic superconducting gap  $\Delta$ , evaluated as a function of temperature for the strained material by 1%, 2%, 4% and 5% strain. In order to estimate  $T_c$  for the anisotropic case, a solid Black line is taken in the center of the lower gap and this line is extrapolated for  $\Delta = 0$  via exponential approximation  $\Delta = \Delta_0 [1 - (T/T_c)^p]^{1/q}$ , with  $\Delta_0$ ,  $p$ ,  $q$  and  $T_c$  being adjustable parameters. The FS is colored in blue and red representing the minimum and maximum values of  $\Delta_k$  at 15 K, respectively corresponding to the color map. Only parts of the Fermi sheet that have  $\Delta_k > 0$  are shown, parts of the Fermi sheet where  $\Delta_k = 0$  are made invisible. The Coulomb parameter used was  $\mu^* = 0.13$ .

### 3 Band structure for the hydrogenated Mo<sub>2</sub>N

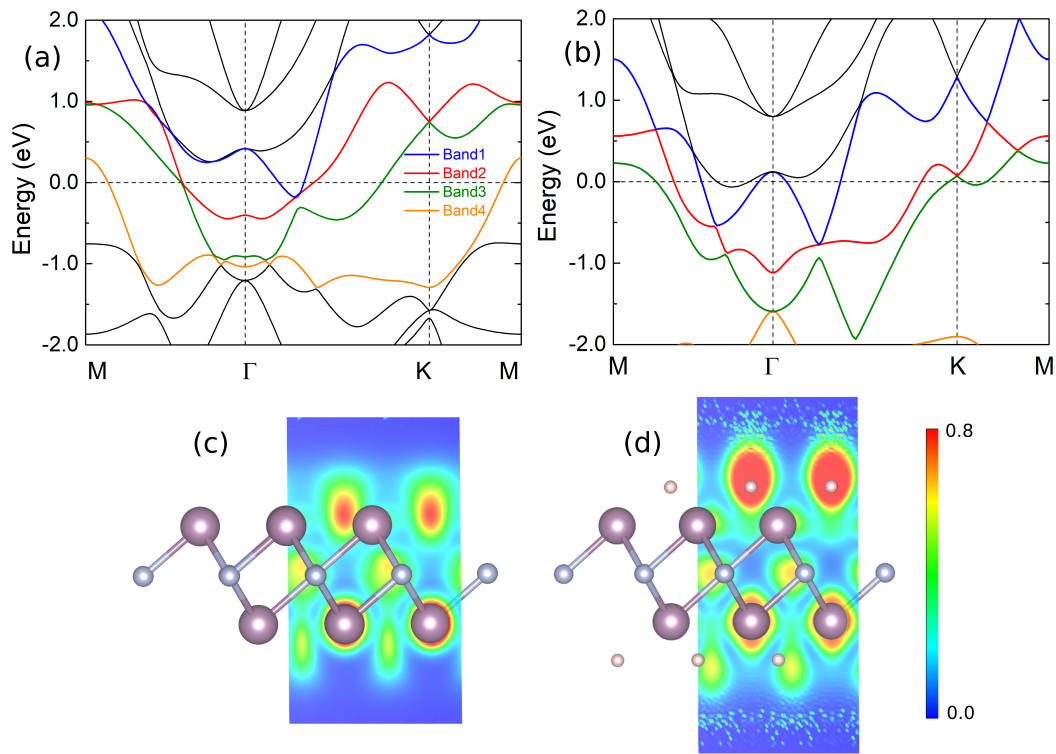


Figure S8: (a) shows the band structure for Mo<sub>2</sub>N relaxed monolayer. (b) shows the band structure for hydrogenated Mo<sub>2</sub>N. The hydrogen atoms are put well above the pockets, in two sides of the monolayer, and the structure is fully relaxed again. (c) and (d) show the ELF color map for Mo<sub>2</sub>N without and with hydrogenation, respectively.

Figure S8a,b shows band structure for pure and hydrogenated Mo<sub>2</sub>N, respectively. As a consequence of the simulated hydrogenation, it was observed a significant changes in the band structure. It occurs mainly in the band4 (orange color) as indicated in Figure S8a, b. For pure Mo<sub>2</sub>N, this band line (in the reciprocal space) is very spread and only crosses the Fermi level at M point, it is associated with localized pockets in the real space. The band4 represents the electron pockets, this hypothesis is corroborated by the new band structure after the hydrogenation. As shown in figure S8c,d, the pockets are strongly bounded by the hydrogen atoms and the band lines associated to this electron pockets tend to stay far way from the Fermi level. This behavior is noted mainly for the Band4 that moves far way from the Fermi level after hydrogenation. The absorbed pockets by hydrogen atoms generate changes in the electronic structure and also impact in the others band lines related to the molybdenum, but this bands keep the original characteristic and continue to cross the Fermi level. In conclusion, the Fermi surface around M point represents the electron pockets, the electron-phonon interaction coming from this part is small compared to the molybdenum 4d electrons.